Int. J. Radiation Oncology Biol. Phys., Vol. 74, No. 2, pp. 575–582, 2009

0360-3016/09/$–see front matter

ELSEVIER

doi:10.1016/j.ijrobp.2008.12.057

PHYSICS CONTRIBUTION

TOWARD SUBMILLIMETER ACCURACY IN THE MANAGEMENT OF INTRAFRACTION MOTION: THE INTEGRATION OF REAL-TIME INTERNAL POSITION MONITORING AND MULTILEAF COLLIMATOR TARGET TRACKING

Amit Sawant, Ph.D.,* Ryan L. Smith, B.S.,† Raghu B. Venkat, M.S.,* Lakshmi Santanam, Ph.D.,† Byungchul Cho, Ph.D.,* Per Poulsen, Ph.D.,* Herbert Cattell, M.S.,‡ Laurence J. Newell, M.S.,§ Parag Parikh, M.D.,† and Paul J. Keall, Ph.D.*

*Stanford Cancer Center, Stanford, CA; †Washington University School of Medicine, St. Louis, MO; ‡Varian Medical Systems, Palo Alto, CA; and §Calypso Medical Technologies, Seattle, WA

Purpose: We report on an integrated system for real-time adaptive radiation delivery to moving tumors. The system combines two promising technologies—three-dimensional internal position monitoring using implanted electromagnetically excitable transponders and corresponding real-time beam adaptation using a dynamic multileaf collimator (DMLC).

Methods and Materials: In a multi-institutional academic and industrial collaboration, a research version of the Calypso position monitoring system was integrated with a DMLC-based four-dimensional intensity-modulated radiotherapy delivery system using a Varian 120-leaf multileaf collimator (MLC). Two important determinants of system performance—latency (*i.e.*, elapsed time between target motion and MLC response) and geometric accuracy—were investigated. Latency was quantified by acquiring continuous megavoltage X-ray images of a moving phantom (with embedded transponders) that was tracked in real time by a circular MLC field. The latency value was input into a motion prediction algorithm within the DMLC tracking system. Geometric accuracy was calculated as the root–mean–square positional error between the target and the centroid of the MLC aperture for patient-derived three-dimensional motion trajectories comprising two lung tumor traces and one prostate trace.

Results: System latency was determined to be approximately 220 milliseconds. Tracking accuracy was observed to be sub-2 mm for the respiratory motion traces and sub-1 mm for prostate motion.

Conclusion: We have developed and characterized a research version of a novel four-dimensional delivery system that integrates nonionizing radiation–based internal position monitoring and accurate real-time DMLC-based beam adaptation. This system represents a significant step toward achieving the eventual goal of geometrically ideal dose delivery to moving tumors.

Adaptive radiotherapy, Intrafraction, Tracking, Motion management.

INTRODUCTION

Modern radiotherapy dose delivery can be performed with submillimeter precision. However, tumor and organ motion during irradiation (intrafraction motion) can cause significant geometric and dosimetric uncertainties (1–4). In its ideal form, radiation delivery in the presence of intrafraction motion has two requirements—complete spatial and temporal knowledge of the irradiated anatomy and continuous adaptation of the radiation beam to account for these spatiotemporal changes. Toward this goal, we recently reported on a real-time three-dimensional (3D) intensity-modulated radiotherapy delivery technique for the management of 3D translational intrafraction motion (5). This method uses an external, optical marker–based real-time position monitoring system (RPM,

Reprint requests to: Amit Sawant, Ph.D., 875 Blake Wilbur Dr., Stanford, CA 94305. Tel: (650) 498-7151; Fax: (650) 498-5008; E-mail: asawant@stanford.edu

This work was supported by research grants from Varian Medical Systems and Calypso Medical Technologies.

Conflict of interest: L.J.N. and H.C. are employees of Calypso Medical Technologies and Varian Medical Systems, respectively. Stanford University receives research funding from Varian Medical Systems.

Acknowledgments—We thank Dr. Shirato from Hokkaido University School of Medicine, Sapporo, Japan, and Drs. Kupelian and Langen from M. D. Anderson Cancer Center, Orlando, FL, for kindly sharing the real-time radiotherapy lung and Calypso prostate motion data, respectively. We also thank Dr. David Carlson, Stanford University, Stanford, CA, for his work in the development of the rotational therapy module of the multileaf collimator tracking algorithm. Thanks to Brian Sargent, Steve Dimmer, Steve Phillips, Luis Retana, and Jay Petersen from Calypso Medical Technologies, Seattle, WA, for providing real-time output capabilities for the Calypso system. Dr. Michelle Svatos from Varian Medical Systems, Palo Alto, CA, deserves special mention for her work in successfully coordinating various scientific and administrative aspects of this multi-institutional effort.

Received Aug 8, 2008, and in revised form Dec 18, 2008. Accepted for publication Dec 19, 2008.

version 1.7; Varian Medical Systems, Palo Alto, CA) to estimate the 3D position of a tumor target and uses this information for online adaptation of the beam aperture via a 120-leaf dynamic multileaf collimator (DMLC) (Varian Medical Systems). This DMLC tracking system has shown submillimeter geometric accuracy in three dimensions and significant improvements in dosimetric accuracy for conformal, intensity-modulated radiotherapy and rotational therapy delivery (5, 6).

Although external markers have been found to be well correlated with internal anatomy within an imaging session (7–9), there is no guarantee that these correlations will continue to exist and be constant throughout the course of the therapy (10). In this respect, implanted radiopaque seeds have been found to be more reliable than external markers (4, 11, 12). However, to obtain high-quality, real-time information about the target from radiopaque markers, it is necessary to perform fluoroscopic X-ray imaging, resulting in increased patient dose; for example, skin dose of up to approximately 2 cGy/min, with a dose at 5 cm of depth ranging from 37% to 58% of peak dose, has been reported for an integrated linear accelerator and fluoroscopic tracking system developed by Shirato *et al.* (13). Furthermore, the American Association of Physicists in Medicine Task Group on Imaging Dose (Task Group no. 75) has estimated the dose to the patient from this system to be up to 14 cGy/min (14).

Recently, a 3D position monitoring system based on electromagnetically excitable implanted markers (*i.e.*, not involving ionizing radiation) has been developed by Calypso Medical Technologies (Seattle, WA). Detailed characterization and clinical demonstration of this system have been reported in the literature (15, 16). The clinical version of this system has been reported to exhibit high accuracy and precision for radiation therapy of the prostate (16). Such accurate localization, the high degree of correlation with the tumor target, and the absence of ionizing radiation (unlike fluoroscopic X-ray imaging of radiopaque fiducials) make this system an attractive choice for accurate real-time position monitoring.

In this work, as part of a multi-institutional academic and industrial collaboration, we report on the integration of real-time DMLC tracking with a research version of the Calypso four-dimensional (4D) localization system (Calypso Medical Technologies). The integrated system is characterized in terms of two important determinants of overall performance—system latency (*i.e.*, elapsed time between target motion and multileaf collimator [MLC] response) and geometric accuracy of DMLC tracking for patient-derived motion traces corresponding to respiratory motion and prostate motion.

METHODS AND MATERIALS

Real-time position monitoring using the Calypso system

The Calypso system monitors position using an electromagnetic planar array to excite and receive signals from three wireless transponders, typically implanted within or near (and therefore spatially correlated with) the tumor target. The current clinical version updates transponder positions at approximately 10 Hz. To enable real-time position monitoring of respiratory motion signals, this clinical version was modified by increasing the update frequency to approximately 25 Hz, sufficiently high so as to adequately sample most respiratory motion (17). Hereafter in this article, unless otherwise stated, the term ''Calypso system'' will refer to this modified research version.

Real-time beam adaptation using DMLC tracking

As part of our research in intrafraction motion management, we have developed a real-time DMLC tracking algorithm based on the Varian 120-leaf Millennium MLC (Varian Medical Systems). The algorithm obtains real-time 3D target location from an independent position monitoring system and dynamically calculates MLC leaf positions as a function of fractional monitor units and 3D position to account for target motion (5). In this study the DMLC tracking software was modified to read real-time target position from the Calypso system. It should be noted that the Calypso system provides positional information at a slightly lower frequency (approximately 25 Hz) than the RPM system (approximately 30 Hz) on which our previous study was based.

Experimental methodology

To characterize the performance of the integrated system, two important properties were investigated—the temporal latency of the system and the geometric accuracy of DMLC tracking. The data flow and the components of the experimental setup are shown in Figs. 1a and 1b, respectively. Target motion was simulated by use of a high-precision (approximately 100 μm), programmable motion platform developed at Washington University, St. Louis, MO (18). Three electromagnetic transponders were embedded into a $10 \times 10 \times 1$–cm^3 solid water slab so as to form an equilateral triangle (in the coronal plane) with the center of the triangle coinciding with that of the slab. A spherical, radiopaque ball bearing (BB) that was approximately 1 mm in diameter was placed at the center of the slab. (Thus each transponder was equidistant from the BB.) The slab was securely fastened to the extended arm of the motion phantom (Fig. 1b), and the entire assembly was placed on the couch of a Varian Trilogy linear accelerator equipped with a 120-leaf DMLC and an electronic portal imaging device (EPID). The DMLC consists of two opposing leaf banks, each comprising 60 leaves. For each bank, the leaf widths, as projected on the isocentric plane (100 cm from the source), are 5 mm and 10 mm for the central (11 to 50) and peripheral leaves (1 to 10 and 51 to 60), respectively. It should be noted that the MLC tracking algorithm uses a strategy of initially fitting virtual ''sub-leaves'' to mitigate the effect of finite leaf width on the spatial accuracy of tracking in the direction perpendicular to leaf motion (5).

The gantry and collimator angles were both set to 90°. The Calypso planar array was positioned directly above the solid water slab as shown in Fig. 1b. The phantom was loaded with mathematically defined sinusoidal as well as patient-derived motion traces, and the instantaneous 3D position calculated by the Calypso system was transmitted via an Ethernet connection to the DMLC tracking computer. The tracking algorithm recalculated MLC leaf positions as a function of dose fraction and target position and sent these leaf positions via a separate Ethernet connection to the MLC controller, which actuated the mechanical movement of the MLC leaves.

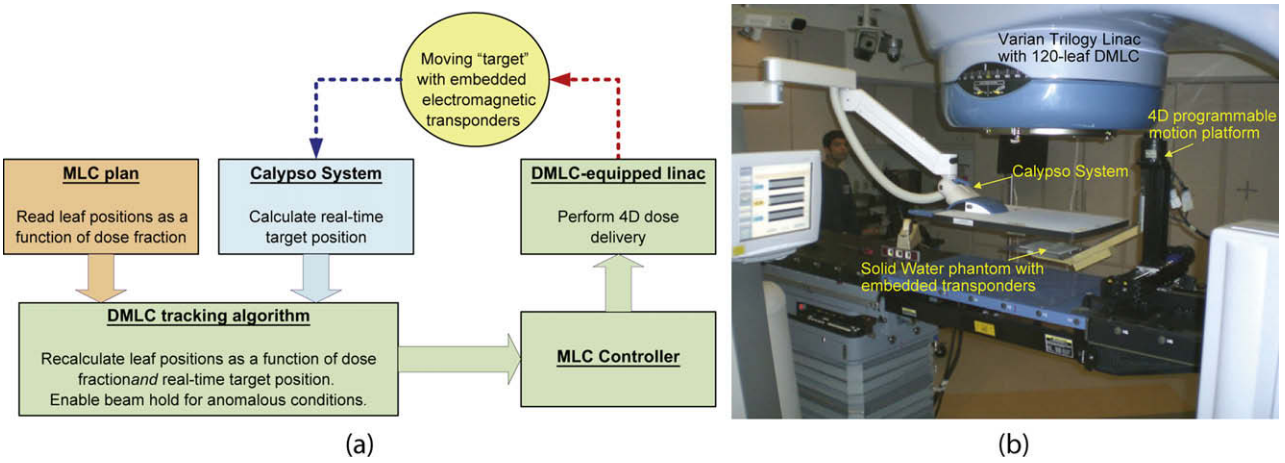

Fig. 1. (a) Workflow of integrated system. (b) Experimental components of geometric accuracy and latency measurements of real-time dynamic multileaf collimator (DMLC) tracking. For the measurements, the gantry was oriented at 90°; it is shown at 180° for a clearer illustration. MLC = multileaf collimator; 4D = four-dimensional; Linac = linear accelerator.

System latency

A finite time lag or latency is observed between motion detection and MLC response. This latency can be attributed to the time taken by each of the subprocesses involved in tracking: motion detection, the calculation of new leaf positions, and the time required by the MLC leaves to reach the physical positions sent by the MLC controller. Latency results in geometric and hence dosimetric errors during dose delivery. To reduce the errors caused by latency, the tracking algorithm uses a modified linear adaptive predictive filter with a user-defined temporal offset equal to the latency to estimate ''future'' target position (19). To determine the magnitude of this latency, the following measurement was performed. The motion platform was programmed with a sinusoidal trajectory (± 1.5 cm, 15 cycles/min) along the direction parallel to MLC motion. The motion of the phantom was tracked by a circular MLC field of 10 cm in diameter at the isocenter. Continuously acquired EPID images at approximately 7 frames per second were used to independently record the tracking process. In an offline analysis the EPID images were semi-interactively segmented to locate the embedded BB ''target'' and the centroid of the MLC aperture in each image frame. The absolute position of the target and the aperture centroid was plotted as a function of elapsed time, and the motion trajectories thus obtained were fitted with sine curves. System latency was calculated from the phase difference between the curves. The calculated latency was used as input to the prediction algorithm for subsequent DMLC tracking measurements. Furthermore, for each set of 3D position data, the Calypso system software also outputs an estimated value of its own latency, which is calculated as the mean time delay between position detection and the output of the estimated 3D position. This self-reported latency of the Calypso system (also output at 25 Hz) was also recorded to decouple the latencies of the position monitoring and beam adaptation components of the entire system.

Geometric accuracy

The geometric accuracy of DMLC tracking of 3D rigid target motion was determined for three patient traces—a respiratory trace showing high variability, recorded by a dual-fluoroscopic real-time radiotherapy (RTRT) system (20); a respiratory trace showing moderate variability, recorded by the Synchrony system (Accuray, Sunnyvale, CA; 21); and a prostate motion trace showing relatively high variability, recorded by the Calypso system (22). Each 3D motion trajectory was programmed into the motion platform. Real-time DMLC tracking of the moving target was performed with the aforementioned 10-cm-diameter circular MLC aperture and recorded via continuous EPID imaging as described in the previous section. The EPID images were segmented, and geometric tracking error was calculated from the positional difference between the trajectories of the target (BB) and the aperture centroid. In each image frame the known value of the diameter of the segmented MLC aperture (10 cm) was used to normalize the pixel spacing to absolute spatial coordinates in the isocentric plane. Consequently, magnification/demagnification of the aperture and the target due to motion along the beam axis was normalized to the isocentric plane. It should be noted that the DMLC tracking algorithm correctly accounts for such motion (5). For each trajectory, the root–mean–square error (RMSE) and the distribution of the positional differences were also calculated.

RESULTS

Figure 2a shows the motion trajectories of the target (red line) and the aperture (blue line) in the absence of prediction. It can be seen that the aperture trajectory systematically lags behind the target trajectory. The system latency corresponding to this lag was estimated to be approximately 220 milliseconds. This value was independently verified by performing the measurement by use of progressively increasing values of the prediction offset, ranging from 0 to 250 milliseconds. The measurement corresponding to the 220-millisecond latency yielded the smallest geometric tracking error. The plots corresponding to the other latency values are not shown, for brevity. All results from this point onward are reported with respect to a latency of 220 milliseconds.

Figure 2b shows a histogram of the temporal latency recorded from the Calypso system. It can be observed that there exists significant variation in the Calypso latency values, with a peak around approximately 90 milliseconds. (As expected, this value is less than the latency of the entire system.) Although the exact cause of this variation is not yet identified, we suspect that there may be at least two contributing factors. First, the software executes three transponder position

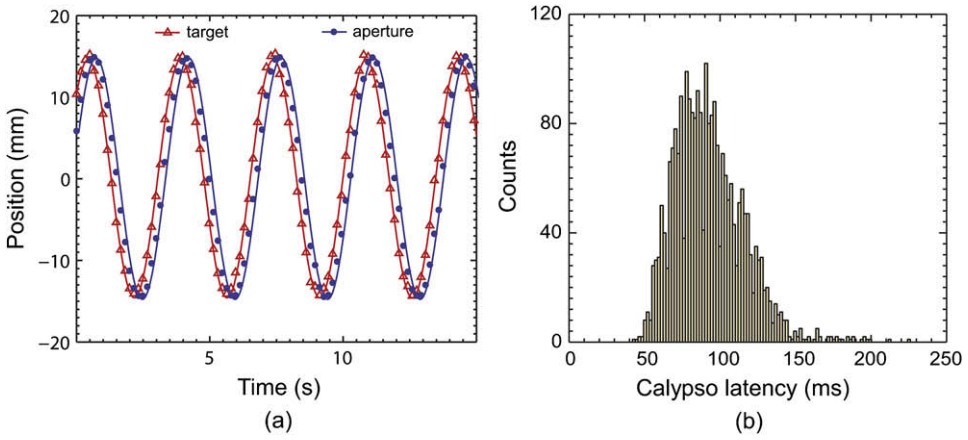

Fig. 2. (a) Target and aperture trajectories without prediction, used to calculate total temporal latency of integrated system. (b) Calypso latency values recorded from system software.

measurements followed by brief system-calibration operations. These calibration operations tend to add a slight computational load on the processor, which in turn may introduce some variability in the timing of the position updates. Second, the operating system (Windows XP; Microsoft Corp., Redmond, WA) on the Calypso computer interleaves measurement processing with other system-related tasks, which may also introduce some variability in the timing of the position updates. It is worthwhile to note that this variation in latency (on the order of tens of milliseconds) will not have any significant impact in the case of prostate treatments, which are the only site currently cleared for clinical use. However, for organs that undergo faster motion (*e.g.*, lung and liver), such variation is important to take into account when real-time beam adaptation strategies such as gating or tracking are used.

Figure 3 shows the components of motion trajectories of the target and the aperture, in directions parallel and perpendicular to the direction of leaf travel, for the two respiratory motion traces (RTRT and Synchrony) and for the prostate motion trace. The tracking error as quantified by the absolute difference between the aperture and the target position is also plotted in each frame (green line). The RTRT lung trace represents a challenging scenario of DMLC tracking, because of target motion that is highly variant and, moreover, comparable in amplitude in both parallel and perpendicular directions to the leaf travel. RMSEs of approximately 1.1 mm and approximately 1.6 mm are observed along the parallel and perpendicular directions, respectively. In both directions errors are particularly pronounced in the peaks and the troughs of the traces, which correspond to transitions between inhale and exhale. These errors are likely a result of over- or under-prediction when target motion is nonlinear and have been reported in the literature for other motion prediction algorithms (23–25). The Synchrony trace represents more commonly observed respiratory motion, where the target moves along an approximately elliptical path. For this trace, the MLC was aligned such that the leaves moved parallel to the major axis of the ellipse. The RMSE for this case is comparable to that observed for the RTRT trace in the parallel direction (approximately 1.4 mm) and significantly less in the perpendicular direction (approximately 0.6 mm). Finally, the Calypso motion trace, which represents a relatively high degree of prostate motion (nevertheless, much slower than respiratory motion), shows tracking error significantly less than 1 mm in both directions.

Figure 4 shows error histograms corresponding to the data shown in Fig. 3. The spread in tracking error appears to be dependent on the nature of the patient trace. Both of the respiratory motion traces exhibit greater spread than the prostate trace. Although the tracking errors lie mostly within approximately 3 mm, there are some instances (*e.g.*, Synchrony lung) where errors as high as 5 mm are observed.

DISCUSSION

The results from these initial studies show the feasibility of real-time 4D MLC-based delivery by use of nonionizing radiation–based internal position monitoring. Sub-2 mm accuracy was observed for moderately varying as well as highly varying respiratory trajectories, showing the robustness of the system in handling a wide range of intrafraction motion. Nevertheless, before such a system achieves clinical realization, there are several factors that must be considered.

For example, the increase in update frequency from 10 to 25 Hz in the research Calypso system results in a corresponding decrease in the total integration period for the three transponder measurements from 100 to 40 milliseconds, which in turn results in a 4-dB reduction in precision (position estimate variance). It should be noted, however, that the accuracy of position estimation using the prototype system (defined as the error in the mean position estimate taken over 30 seconds of localization) is unlikely to be affected due to the fact that, with the higher update frequency, 2.5 times as many samples are acquired in these 30 seconds. We are currently exploring strategies to recover the 4-dB degradation in precision.

In the case of the respiratory traces, the integrated system exhibited sub-2 mm RMSEs in tracking. Interestingly,

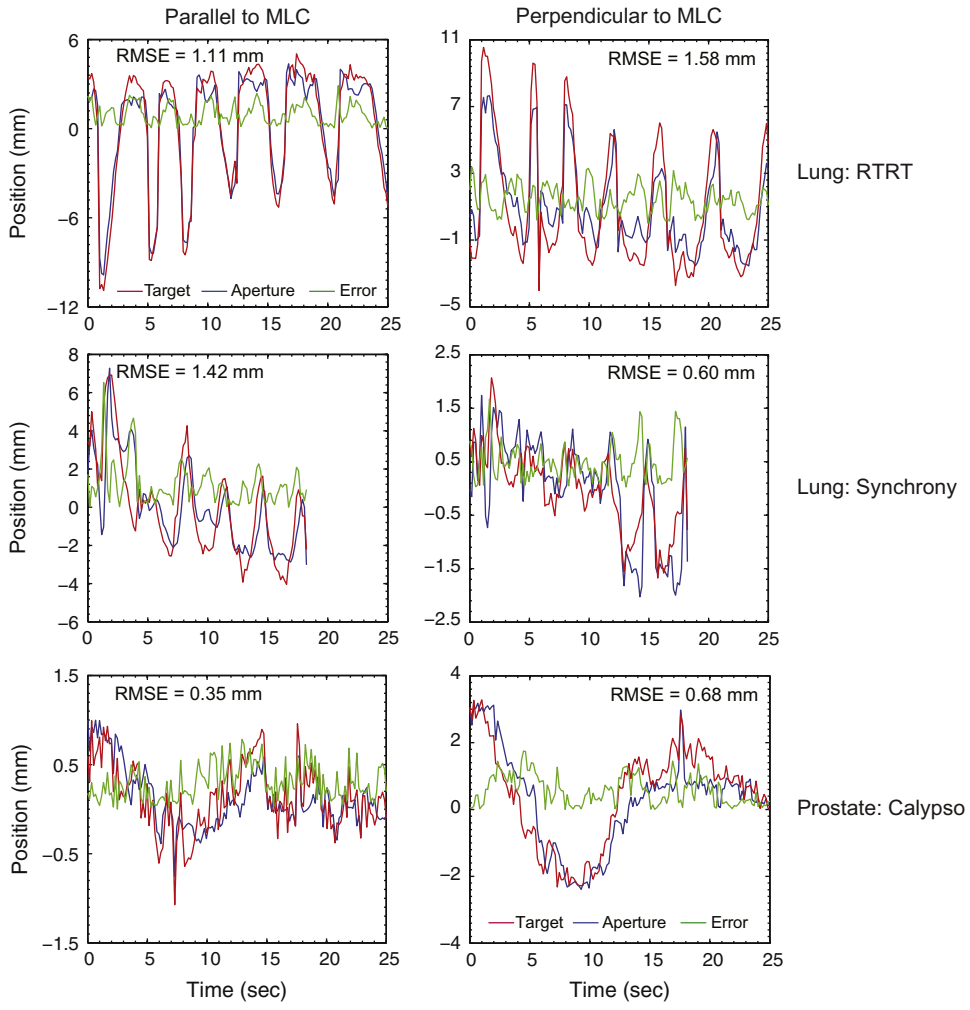

Fig. 3. Geometric accuracy of dynamic multileaf collimator tracking of target motion parallel (left column) and perpendicular (right column) to multileaf collimator (MLC) leaf motion in the beam's-eye view. Motion trajectories of the target (red line) and the MLC aperture (blue line) are shown for highly variant respiratory motion (real-time radiotherapy [RTRT]) (top row), moderately variant respiratory motion (Synchrony) (middle row), and relatively large prostate motion (Calypso) (bottom row). The green line in each figure indicates the tracking error. The corresponding root–mean–square error (RMSE) is given in each panel.

previous measurements of tracking error using the RPM system for position monitoring have yielded sub-1 mm accuracy in all three directions (5). The relatively higher error observed with Calypso-based DMLC tracking is likely attributed to two factors. First, the current implementation of the prediction algorithm assumes a constant value for temporal latency. The variable latency of the Calypso system (Fig. 2b) reduces the accuracy of the prediction algorithm. Second, the predictive power of the algorithm decreases as the latency increases. As a result, the relatively higher overall latency of the Calypso-based DMLC tracking system, approximately 220 milliseconds [compared with approximately 160 milliseconds for the RPM-based system (26)], results in greater prediction errors. It is expected that improvements in software design and the speed of processing hardware will likely reduce both the magnitude and the spread in temporal latency and therefore the resultant error. An alternate strategy is to modify the prediction algorithm so as to accept variable values for the temporal offset. Finally, it is important to note that the two systems measure different things: the RPM system is an external surrogate of tumor motion, whereas the Calypso system is an internal surrogate. This study does not address the relative merits of these approaches for lung tumor tracking.

Although the implantation of Calypso transponders has been shown clinically for the prostate (22), these transponders (cylindrical, 8.5 mm in length, and 1.8 mm in diameter) (15) are significantly larger than typical radiopaque fiducials [cylindrical, 3 mm in length, and 0.8 mm in diameter (27, 28) or spherical and 2 mm in diameter (29, 30)] implanted in the lungs. Percutaneous implantation of fiducials in the lung has led to a significant rate of pneumothoraces (27). Bronchoscopic implantation of fiducials has been safer but has not become part of routine clinical practice in most centers (31, 32). Thus the safety and efficacy of these transponders and potential design modifications for respiratory monitoring need to

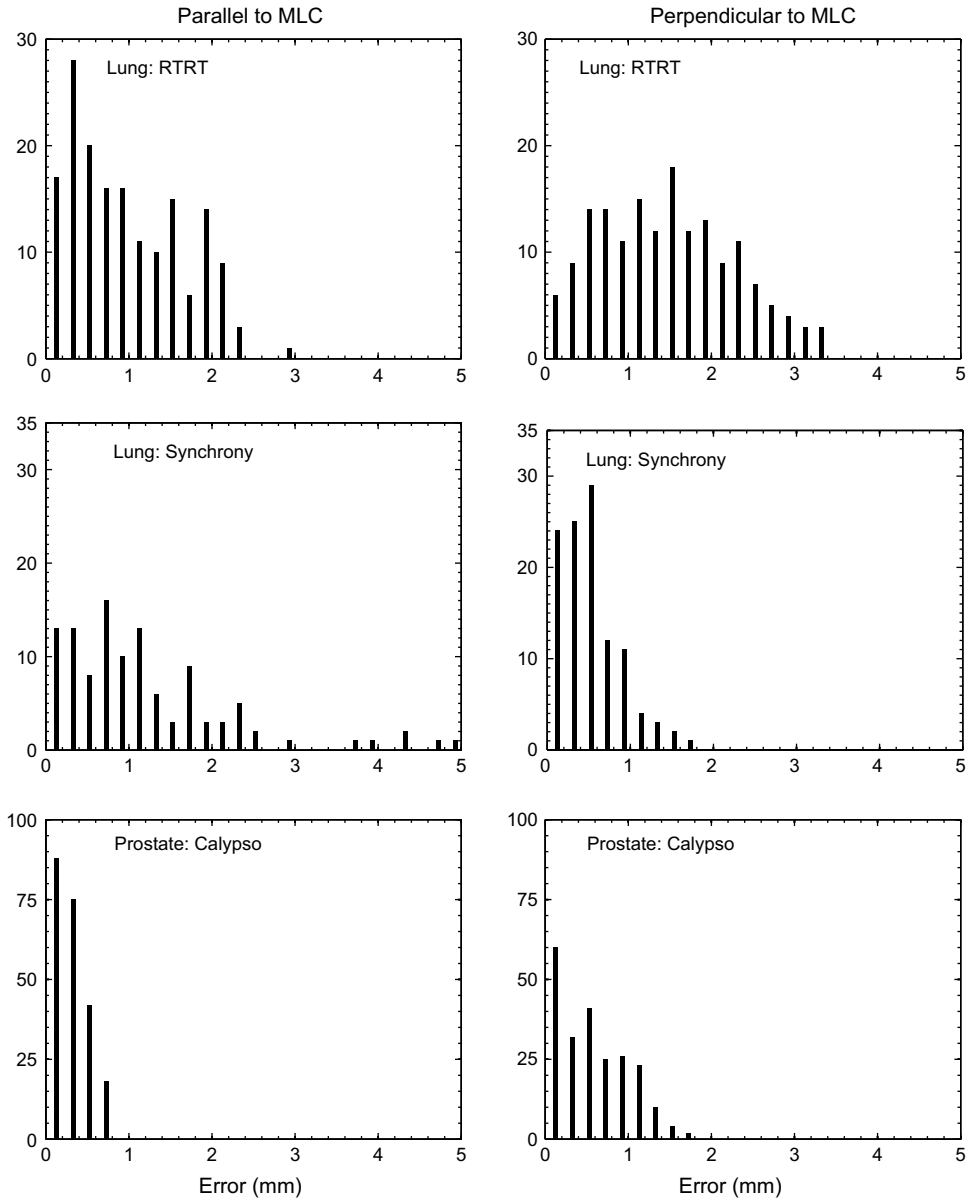

Fig. 4. Distribution of geometric tracking errors for traces shown in Fig. 3. MLC = multileaf collimator; RTRT = real-time radiotherapy.

be carefully examined. Toward this end, investigators at Washington University are studying the feasibility and stability of bronchoscopic implantation of transponders into canine lungs. Early studies have shown that the present design of Calypso transponders (such as those used in this work) show good to moderate short-term but low long-term fixation rates (33). However, in a more recent study using an improved, ''non-migrating'' transponder design, 100% fixation rates over a 60-day period were reported for 54 bronchoscopically implanted transponders (nine per animal) (34).

Interfraction transponder migration and intrafraction transponder migration are other potential concerns, particularly for implantation within the lung. The transponders used in the Calypso system have shown long-term positional stability, comparable to that of radiopaque markers in the prostate (35) and the lung (33). Although these long-term studies do not seem to indicate a significant possibility of intrafraction migration, this effect nevertheless needs to be investigated separately.

In its current form the integrated system performs 4D delivery to a single point (typically the target centroid) undergoing rigid translational motion. It is also theoretically possible to estimate in-plane rigid rotation. Toward this end, preliminary studies are under way at Washington University to estimate prostate rotation from real-time Calypso data (36).

To account for more complex motion and, potentially, dissimilar motion of multiple targets, significant modifications may be required on both the position monitoring and the delivery components of the system. For example, whereas each of the three electromagnetic transponders independently provides real-time 3D position information, the update frequency of an individual transponder is approximately one-third of 25 Hz. For three transponders placed in close

proximity to a single target, this update rate is adequate to temporally sample target motion due to respiration. However, higher update frequencies may be required to monitor multiple targets in the lung. Furthermore, for monitoring more complex motion such as deformation, strategies that use more than three transponders may be required.

On the delivery side, the fact that each MLC leaf is controlled independently means that each leaf can be considered a degree of freedom for repositioning and reoptimization. Thus, if real-time information about the shape of the target as seen in the beam's-eye view is made available to the tracking algorithm, then, as a first approximation, the instantaneous fluence map can be modified so as to conform to the new shape. Furthermore, theoretic investigations of other sophisticated approaches of realigning the leaves to account for translational as well as more complex target motion have been described in the literature (37–42).

Finally, it is important to note that geometric tracking accuracy is not a margin recipe. The sub-2 mm accuracy reported in this work represents, purely, the technical capability of the integrated system. In addition to target motion, clinical margins have to account for several other sources of error such as uncertainties in gross tumor volume/clinical target volume delineation, anatomic changes between pretreatment imaging and treatment delivery, errors in patient localization from session to session, and uncertainties resulting from physiologic factors such as changes in the respiratory pattern, filling of the bladder (compared with the state during pretreatment imaging), and so on. The contribution of real-time tracking toward margin reduction is related only to target motion; errors resulting from other uncertainties have to be minimized independently for further margin reduction.

In summary, the integration of non-irradiating internal position monitoring and real-time beam adaptation represents a significant step toward the eventual goal of target volume–based image guidance for intrafraction motion management. Further studies will involve addressing the issues outlined previously, including estimating and accounting for more complex forms of motion such as target rotation and deformation.

REFERENCES

1. Huang E, Dong L, Chandra A, *et al*. Intrafraction prostate motion during IMRT for prostate cancer. *Int J Radiat Oncol Biol Phys* 2002;53:261–268.
2. George R, Keall PJ, Kini VR, *et al*. Quantifying the effect of intrafraction motion during breast IMRT planning and dose delivery. *Med Phys* 2003;30:552–562.
3. Hugo G, Tenn S, Agazaryan N. An evaluation of intrafraction motion-induced error for fractionated IMRT delivery. *Med Phys* 2003;30:1470–1470.
4. Keall PJ, Mageras GS, Balter JM, *et al*. The management of respiratory motion in radiation oncology report of AAPM Task Group 76. *Med Phys* 2006;33:3874–3900.
5. Sawant A, Venkat R, Srivastava V, *et al*. Management of three-dimensional intrafraction motion through real-time DMLC tracking. *Med Phys* 2008;35:2050–2061.
6. Zimmerman J, Korreman S, Persson G, *et al*. DMLC motion tracking of moving targets for intensity modulated arc therapy treatment—A feasibility study. *Acta Oncol* 2008;1–6.
7. Beddar AS, Kainz K, Briere TM, *et al*. Correlation between internal fiducial tumor motion and external marker motion for liver tumors imaged with 4D-CT. *Int J Radiat Oncol Biol Phys* 2007;67:630–638.
8. Gierga DP, Brewer J, Sharp GC, *et al*. The correlation between internal and external markers for abdominal tumors: Implications for respiratory gating. *Int J Radiat Oncol Biol Phys* 2005;61: 1551–1558.
9. Yan H, Yin FF, Zhu GP, *et al*. The correlation evaluation of a tumor tracking system using multiple external markers. *Med Phys* 2006;33:4073–4084.
10. Jiang SB. Radiotherapy of mobile tumors. *Semin Radiat Oncol* 2006;16:239–248.
11. Kitamura K, Shirato H, Shimizu S, *et al*. Registration accuracy and possible migration of internal fiducial gold marker implanted in prostate and liver treated with real-time tumor-tracking radiation therapy (RTRT). *Radiother Oncol* 2002;62:275–281.
12. Shirato H, Harada T, Harabayashi T, *et al*. Feasibility of insertion/implantation of 2.0-mm-diameter gold internal fiducial markers for precise setup and real-time tumor tracking in radiotherapy. *Int J Radiat Oncol Biol Phys* 2003;56:240–247.
13. Shirato H, Oita M, Fujita K, *et al*. Feasibility of synchronization of real-time tumor-tracking radiotherapy and intensity-modulated radiotherapy from viewpoint of excessive dose from fluoroscopy. *Int J Radiat Oncol Biol Phys* 2004;60:335–341.
14. Murphy MJ, Balter J, Balter S, *et al*. The management of imaging dose during image-guided radiotherapy: Report of the AAPM Task Group 75. *Med Phys* 2007;34:4041–4063.
15. Balter JM, Wright JN, Newell LJ, *et al*. Accuracy of a wireless localization system for radiotherapy. *Int J Radiat Oncol Biol Phys* 2005;61:933–937.
16. Willoughby TR, Kupelian PA, Pouliot J, *et al*. Target localization and real-time tracking using the Calypso 4D localization system in patients with localized prostate cancer. *Int J Radiat Oncol Biol Phys* 2006;65:528–534.
17. Seppenwoolde Y, Berbeco RI, Nishioka S, *et al*. Accuracy of tumor motion compensation algorithm from a robotic respiratory tracking system: A simulation study. *Med Phys* 2007;34:2774–2784.
18. Malinowski K, Lechleiter K, Hubenschmidt J, *et al*. Use of the 4D phantom to test real-time targeted radiation therapy device accuracy. *Med Phys* 2007;34:2611–2611.
19. Srivastava V, Keall PJ, Sawant A, *et al*. Accurate prediction of intra-fraction motion using a modified linear adaptive filter. *Med Phys* 2007;34:2546.
20. Shimizu S, Shirato H, Ogura S, *et al*. Detection of lung tumor movement in real-time tumor-tracking radiotherapy. *Int J Radiat Oncol Biol Phys* 2001;51:304–310.
21. Suh Y, Dieterich S, Cho B, *et al*. An analysis of thoracic and abdominal tumour motion for stereotactic body radiotherapy patients. *Phys Med Biol* 2008;53:3623–3640.
22. Kupelian P, Willoughby T, Mahadevan A, *et al*. Multi-institutional clinical experience with the Calypso System in localization and continuous, real-time monitoring of the prostate gland during external radiotherapy. *Int J Radiat Oncol Biol Phys* 2007;67:1088–1098.
23. Murphy MJ, Dieterich S. Comparative performance of linear and nonlinear neural networks to predict irregular breathing. *Phys Med Biol* 2006;51:5903–5914.
24. McCall KC, Jeraj R. Dual-component model of respiratory motion based on the periodic autoregressive moving average (periodic ARMA) method. *Phys Med Biol* 2007;52:3455–3466.
25. Ruan D, Fessler JA, Balter JM. Real-time prediction of respiratory motion based on local regression methods. *Phys Med Biol* 2007;52:7137–7152.

26. Wijesooriya K, Bartee C, Siebers JV, *et al*. Determination of maximum leaf velocity and acceleration of a dynamic multileaf collimator: Implications for 4D radiotherapy. *Med Phys* 2005; 32:932–941.
27. Whyte RI, Crownover R, Murphy MJ, *et al*. Stereotactic radiosurgery for lung tumors: Preliminary report of a phase I trial. *Ann Thorac Surg* 2003;75:1097–1101.
28. Le QT, Loo BW, Ho A, *et al*. Results of a phase I dose-escalation study using single-fraction stereotactic radiotherapy for lung tumors. *J Thorac Oncol* 2006;1:802–809.
29. Seppenwoolde Y, Shirato H, Kitamura K, *et al*. Precise and real-time measurement of 3D tumor motion in lung due to breathing and heartbeat, measured during radiotherapy. *Int J Radiat Oncol Biol Phys* 2002;53:822–834.
30. Shirato H, Shimizu S, Kunieda T, *et al*. Physical aspects of a real-time tumor-tracking system for gated radiotherapy. *Int J Radiat Oncol Biol Phys* 2000;48:1187–1195.
31. Kupelian PA, Forbes A, Willoughby TR, *et al*. Implantation and stability of metallic fiducials within pulmonary lesions. *Int J Radiat Oncol Biol Phys* 2007;69:777–785.
32. Imura M, Yamazaki K, Kubota KC, *et al*. Histopathologic consideration of fiducial gold markers inserted for real-time tumor-tracking radiotherapy against lung cancer. *Int J Radiat Oncol Biol Phys* 2008;70:382–384.
33. Mayse ML, Parikh PJ, Lechleiter KM, *et al*. Bronchoscopic implantation of a novel wireless electromagnetic transponder in the canine lung: A feasibility study. *Int J Radiat Oncol Biol Phys* 2008.
34. Mayse ML, Smith RL, Park M, *et al*. Development of a non-migrating electromagnetic transponder system for lung tumor tracking. *Int J Radiat Oncol Biol Phys* 2008;72:S430–S430.
35. Litzenberg DW, Willoughby TR, Balter JM, *et al*. Positional stability of electromagnetic transponders used for prostate localization and continuous, real-time tracking. *Int J Radiat Oncol Biol Phys* 2007;68:1199–1206.
36. Noel C, Parikh P, Santanam L. Analysis of the effect of prostate rotation on target coverage usingusing real-time tracking technology. *Proceedings of the 10th International Workshop on Electronic Portal Imaging and Positioning Devices*, San Francisco, CA, 2008. p. 98–99.
37. Papiez L, Rangaraj D, Keall P. Real-time DMLC IMRT delivery for mobile and deforming targets. *Med Phys* 2005;32: 3037–3048.
38. Webb S, Binnie DM. A strategy to minimize errors from differential intrafraction organ motion using a single configuration for a 'breathing' multileaf collimator. *Phys Med Biol* 2006;51: 4517–4531.
39. McQuaid D, Webb S. IMRT delivery to a moving target by dynamic MLC tracking: Delivery for targets moving in two dimensions in the beam's eye view. *Phys Med Biol* 2006;51:4819–4839.
40. McMahon R, Papiez L, Rangaraj D. Dynamic-MLC leaf control utilizing on-flight intensity calculations: A robust method for real-time IMRT delivery over moving rigid targets. *Med Phys* 2007;34:3211–3223.
41. McClelland JR, Webb S, McQuaid D, *et al*. Tracking 'differential organ motion' with a 'breathing' multileaf collimator: Magnitude of problem assessed using 4D CT data and a motion-compensation strategy. *Phys Med Biol* 2007;52:4805–4826.
42. Tacke M, Nill S, Oelfke U. Real-time tracking of tumor motions and deformations along the leaf travel direction with the aid of a synchronized dynamic MLC leaf sequencer. *Phys Med Biol* 2007;52:N505–N512.